JOURNAL OF MATERIALS SCIENCE 30 (1995) 1397–1404

# *In-situ* electrical resistivity measurements: study of magnetic and phase transitions and solid–HDDR processes in Nd–Fe–B-type alloys

O. GUTFLEISCH, I. R. HARRIS
*School of Metallurgy and Materials Science, University of Birmingham, Birmingham B15 2TT, UK*

Nd–Fe–B-type alloys have been characterized by means of *in-situ* electrical resistivity measurements. The potential of this technique for monitoring various phenomena relevant to the hydrogenation, disproportionation, desorption and recombination (HDDR) processing of Nd–Fe–B-type alloys is assessed, together with an evaluation of its capacity for delineating magnetic and phase transitions. The effects of external parameters, such as hydrogen pressure and processing temperature, and of intrinsic parameters, such as alloy composition and initial microstructure, on the kinetics of the solid–HDDR process have been investigated. It was found that the amount of neodymium-rich intergranular phase present in the material had a significant influence on the rates of disproportionation and recombination reactions. At 620 °C, the recombination process takes place as a solid–solid reaction, and this has a marked effect on the reaction rate. It was also found that the disproportionation process is very sensitive to the hydrogen pressure and the dependence of the overall process on the processing temperature between 620 and 900 °C has been determined.

## 1. Introduction

Electrical resistivity measurements are an effective and sensitive means of monitoring various phenomena relevant to the characterization and processing of rare-earth transition metal alloys and magnets. Previous work in this laboratory (see, for example [1, 2]) has shown that the precipitation hardening in $Sm_2(TM)_{17}$-type alloys can be monitored using electrical resistivity measurements. Previous work has also shown that *in situ* electrical resistivity measurements can be used to monitor magnetic and phase transitions [3], the homogenization behaviour [4] and the kinetics of the hydrogenation, disproportionation, desorption and recombination (HDDR) process [3] of Nd–Fe–B-type alloys.

The HDDR process has been reported as a method of producing highly coercive powder via a hydrogen-induced structural change and this powder can be used for the production of Nd–Fe–B-type hot-pressed and bonded hard magnets [5, 6]. The process consists of hydriding the material, then heating the hydrided alloy to $\sim 800\,^{\circ}C$. After holding at this temperature for approximately 2 h, the material is out-gassed in a vacuum again at $\sim 800\,^{\circ}C$ and allowed to cool to room temperature. The first stage, heating under a hydrogen atmosphere, results in the decrepitation of the ingot which is described as the HD process [7]. The initial hydriding process takes place in two steps. First, reaction between the neodymium-rich phase and hydrogen results in the formation of $NdH_{\sim 3}$ and second, the $Nd_2Fe_{14}B$ matrix phase forms a solution $Nd_2Fe_{14}BH_{\sim 2.8}$. The disproportionation reaction then occurs at elevated temperatures and results in the formation of an intimate mixture of α-Fe, neodymium-hydride ($NdH_{\sim 2.2}$) and $Fe_2B$. On desorbing the hydrogen, the remaining constituents recombine to form the thermodynamically more stable $Nd_2Fe_{14}B$ phase. The main microstructural feature of the HDDR process is the conversion of the coarse-grained $Nd_2Fe_{14}B$ phase into a material with submicrometre grain size. Recent work has shown that complex diffusion mechanisms take place during the different stages of the HDDR process [8, 9].

The HDDR kinetics depend on external parameters such as the hydrogen pressure and the processing temperature and on intrinsic parameters such as the alloy composition and the initial microstructure, where the effect of additional elements and the amount and distribution of neodymium-rich phase have to be considered. The reaction kinetics can be monitored by means of *in situ* electrical resistivity measurements of the non-decrepitated material by introducing the hydrogen at elevated temperatures ($T \sim 800\,^{\circ}C$). Disproportionation occurs during hydrogenation with the consequent absence of cracking. This type of reaction can be referred to as "solid–HDDR" [8].

The present work summarizes the electrical resistivity studies carried out on Nd–Fe–B-type alloys and focuses on the HDDR process.

0022–2461 © *1995 Chapman & Hall*

## 2. Experimental procedure

A variety of Nd–Fe–B-type alloys with different additions have been investigated by means of *in situ* electrical resistivity measurements. A stoichiometric (homogenized $Nd_2Fe_{14}B$) and a "Neomax"-type (as-cast and homogenized $Nd_{16}Fe_{76}B_8$) ternary alloy were chosen, as well as a copper-containing alloy (as-cast $Nd_{15.6}Fe_{74.9}B_8Cu_{1.5}$) which is known [10] to exhibit a significantly lowered melting point of the neodymium-rich intergranular phase and an alloy with various additions (as-cast $Nd_{14.68}Dy_{0.94}Al_{0.62}Fe_{76.47}Nb_{0.5}B_{6.79}$) which is used for the commercial production of magnets.

The resistivity measurement employed is based on the standard four-probe method. The potential was measured in the forward and reverse directions to eliminate thermal e.m.f. contributions. The apparatus consists of an on-line data acquisition unit controlling a switch-box, a digital micro-voltmeter and a temperature-compensated reference resistor. It is possible to use this system as a rapid means of characterizing the material at room temperature or as a means of measuring the resistivity *in situ* during a heat treatment up to 1000 °C in a non-inductively wound furnace under vacuum, argon, nitrogen or hydrogen atmosphere. The absorption and desorption behaviour is monitored with a pressure transducer and a Penning gauge, respectively. To provide a supply of pure hydrogen, a $LaNi_5$ hydrogen store is used. The hydrogen is connected to the system via a needle valve and a micrometer filter prevents fine powder contaminating the system. The attachment of the very fine wires on parallelepiped shaped samples, of small dimensions ( $\sim 0.8$ mm $\times$ 8 mm $\times$ 15 mm, $m \sim 0.7$ g) and of high intrinsic brittleness, which were cut from the bulk material, is achieved using a micro-spotwelder which was especially constructed for this purpose. The electric circuit of the micro-spotwelder includes a thyristor, which acts as a switch and enables the capacitor to discharge through the specimen. The spotwelding conditions need to be modified depending upon the sample material. Important factors are the sample thickness and sample surface preparation, the weight of the electrode, the discharge voltage, the spotwelding atmosphere and especially the wire material. For the *in situ* measurements of the electrical resistivity, the spotwelded contacts need to be stable up to 1000 °C. For measurements in this temperature range, a combination of thin stainless steel strips and copper-wire was employed. For monitoring the HDDR process, the samples were heated under vacuum (the chamber was initially evacuated to $10^{-6}$ mbar) to elevated temperatures ($T = 620$–$900$ °C) and then hydrogen was introduced into the system ($p(H_2) = 0.1$–$1.0$ bar). The samples were usually exposed to hydrogen for 2 h and were held for another 2 h under vacuum to allow the sample to desorb fully and recombine. The applied heating rate was 5 °C min$^{-1}$ and the measurements were taken at temperature intervals of 2 °C or at isotherms, every 30 s. It is important to note that the desorption/recombination process is sensitive to the pumping speed, which has to be kept constant when investigating the reaction rates.

By far the largest errors involved in the present measurements were the determination of the specimen dimensions, and the distance between the potential leads. Another factor is the spotwelding procedure itself which gives rise to some uncertainty as the fusion process can vary slightly from sample to sample. For these reasons the absolute resistivities are subject to an error of approximately $\pm$ 5%, although the results from a particular sample are reproducible within themselves to better than $\pm$ 1%.

## 3. Results and discussion

### 3.1. Magnetic and phase transitions

Typical normalized resistivity $\rho/\rho_0$ ($\rho_0$ is the resistivity at room temperature) behaviours of the alloys $Nd_{14.68}Dy_{0.94}Al_{0.62}Fe_{76.47}Nb_{0.5}B_{6.79}$ and $Nd_{15.6}Fe_{74.9}B_8Cu_{1.5}$ during heating under vacuum are shown in Fig. 1. The electrical resistivity exhibits an anomalous behaviour when changes in magnetic ordering occur and the Curie point resistance anomaly is delineated clearly in Fig. 1. For anisotropic material such as $Nd_2Fe_{14}B$, the direction of current flow has to be specified in relation to the crystal axes. The present measurements were carried out approximately parallel to the *a*, *b*-plane of the cast material. The extent of the Curie-point anomaly for the two alloys could be due to a different degree of anisotropy present in the ingot material introduced during the production process. The slope changes in the resistivity curves for the $Nd_{14.68}Dy_{0.94}Al_{0.62}Fe_{76.47}Nb_{0.5}B_{6.79}$ alloy at $T = 650 \pm 3$ °C and for the $Nd_{15.6}Fe_{74.9}B_8Cu_{1.5}$ alloy at $T = 482 \pm 3$ °C can be attributed to the formation of the liquid phase at the grain boundaries, and these temperatures are in good agreement with those obtained by Schneider *et al.* [11] for the former and by Mueller *et al.* [10] for the latter, from DTA studies.

### 3.2. Overall HDDR process

A schematic diagram for a HDDR experiment (including heating and cooling) monitored by measuring the electrical resistivity (first cycle) is shown in Fig. 2. Resistivity, hydrogen absorption and desorption pressures and temperature are shown versus time. The samples were heated under vacuum to elevated temperatures ($T \simeq 800$ °C) and then hydrogen was introduced into the system ($p(H_2) = \sim 0.7$ bar). During heating and cooling the Curie-point resistance anomaly and phase (melting/solidification of neodymium-rich grain-boundary phase) transitions are delineated. The rapid decrease in resistivity after the introduction of hydrogen corresponds to the disproportionation process, which can be described [12] at $T = 750$ °C as

$$Nd_2Fe_{14}B + 2 \pm xH_2 \rightleftharpoons 2NdH_{2\pm x} + 12Fe + Fe_2B \quad (1)$$

(with $x$ as a function of hydrogen pressure and temperature).

After an initial peak in resistivity due to the hydrogenation of the neodymium-rich grain-boundary phase (see Section 3.3), the significant decrease in resistivity can be attributed mainly to the formation of

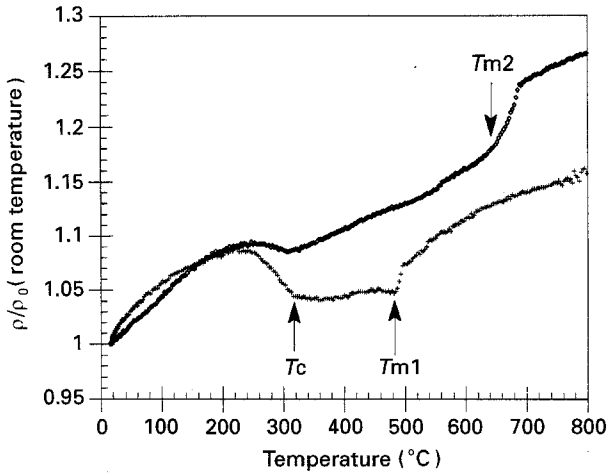


*Figure 1* Electrical resistivity versus time monitoring the magnetic and phase transition in a $Nd_{15.6}Fe_{74.9}B_8Cu_{1.5}$; ((+) alloy 1, $T_C = 312 \pm 3\,°C$) and $Nd_{14.68}Dy_{0.94}Al_{0.62}Fe_{76.47}Nb_{0.5}B_{6.79}$ ((◆) alloy 2, $T_C = 310 \pm 3\,°C$).

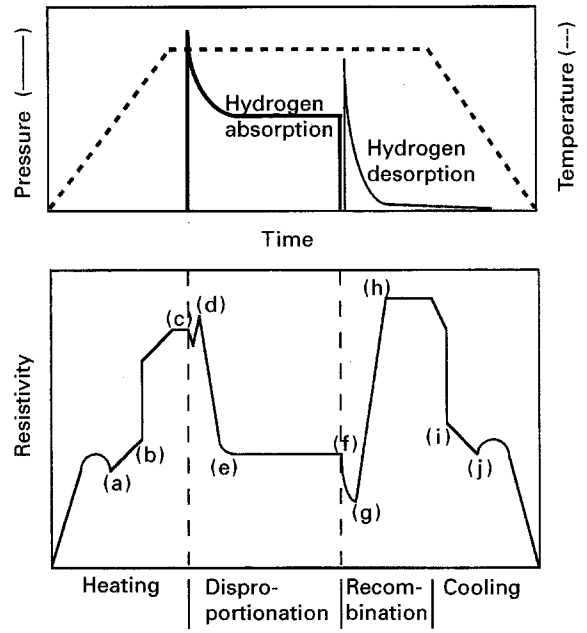


*Figure 2* Schematic diagram for a complete HDDR experiment (including heating and cooling) monitored by measuring the electrical resistivity: (a) Curie-point on heating, (b) grain-boundary melting, (c) onset of disproportionation, (d) hydrogenation of the neodymium-rich phase, (e) completion of disproportionation, (f) dissociation of neodymium hydride, (g) recombination to form $Nd_2Fe_{14}B$, (h) completion of recombination, (i) grain-boundary solidification, (j) Curie-point on cooling.

free iron. Another contribution arises from the formation of the neodymium hydride. The equilibrium value of resistivity after disproportionation depends upon the hydrogen pressure in the system (see Section 3.6). On evacuating the system, the $NdH_{2\pm x}$ phase desorbs and the sudden decrease in resistivity can be attributed to the dissociation of neodymium hydride into neodymium which subsequently recombines with the other constituents. Thus the intimate mixture of iron, ferro-boron and neodymium becomes thermodynamically unstable and recombines to form the more stable $Nd_2Fe_{14}B$ phase resulting in an increase in resistivity. The increase in resistivity after recombination compared with that before disproportionation could be due to enhanced scattering of electrons at the boundaries of the now submicrometre sized grains. Prolonged recombination at high temperature is known to cause extensive grain growth within the reformed $Nd_2Fe_{14}B$ phase [13]. However, the resistivity measurement is not particularly sensitive to that phenomenon.

## 3.3 The role of the neodymium-rich intergranular phase

Fig. 3 shows the isothermal part of the electrical resistivity versus time, which delineates the S-HDDR process at $T = 800\,°C$ and $p(H_2) = 0.7$ bar for the as-cast $Nd_{16}Fe_{76}B_8$ and the stoichiometric $Nd_2Fe_{14}B$ alloy. It can be seen that the disproportionation and recombination reaction rates are higher for the $Nd_{16}Fe_{76}B_8$ alloy. Shortly after the introduction of hydrogen, a small maximum (see insert in Fig. 3) in the resistivity curve of the $Nd_{16}Fe_{76}B_8$ alloy can be observed, and this can be related to the rapid hydrogenation of the neodymium-rich grain boundary resulting in the formation of $NdH_{2\pm x}$. For the stoichiometric alloy, no initial maximum in resistivity after the introduction of hydrogen is observed, consistent with the absence of the neodymium-rich grain-boundary phase in this alloy.

In Fig. 4 it is shown that the hydrogenation of the grain-boundary phase results in the solidification of this phase, which has its melting point at $T = 650\,°C$ [11]. The change in slope in the resistivity trace corresponds to the melting of the intergranular neodymium-rich material during heating in vacuum. The material was then disproportionated at 800 °C causing a drop in resistivity. Cooling the disproportionated $Nd_{16}Fe_{76}B_8$ alloy from 800 °C results in a regular

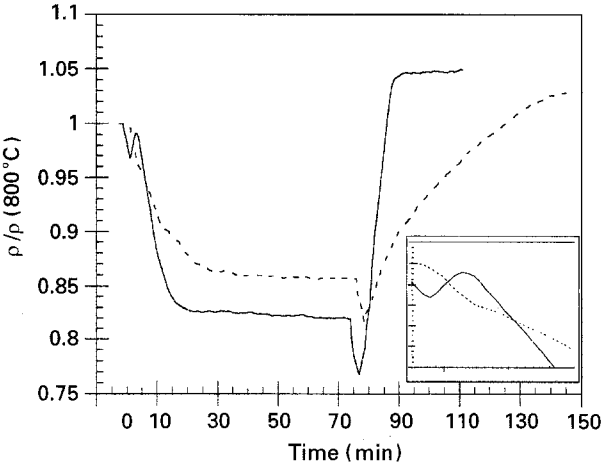


*Figure 3* Isothermal part of the electrical resistivity versus time monitoring the S-HDDR process at $T = 800\,°C$ and $p(H_2) = 0.7$ bar for (—) an as-cast $Nd_{16}Fe_{76}B_8$ and (– – –) a stoichiometric $Nd_2Fe_{14}B$ alloy (hydrogen introduction at $t = 0$ min, evacuation of the system at $t = 75$ min). Insert shows the initial variations in more detail.

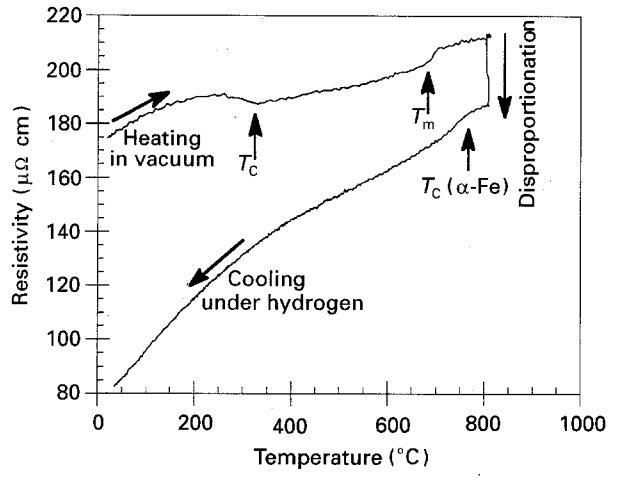


*Figure 4* Heating of a $Nd_{16}Fe_{76}B_8$ as-cast alloy under vacuum, disproportionation at 800 °C and cooling of the disproportionated mixture under hydrogen showing the absence of a solidification reaction of the neodymium-rich phase.

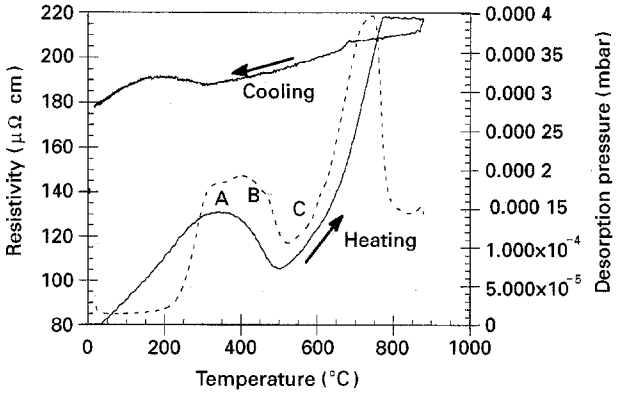


*Figure 5* (——) Resistance and (– – –) desorption behaviour on reheating the disproportionated mixture under vacuum; pressure changes indicate the transition of $NdH_{\sim 2.7}$ to $NdH_{\sim 2}$ of the neodymium-rich phase (A), the disproportionated matrix phase (B), and the start of recombination reaction (C).

decrease in resistivity, indicative of the absence of a solidification reaction consistent with the intergranular phase being in the hydrided and solid state. The small kink around 770 °C in the cooling curve could be attributed to the Curie-point of α-Fe, which is a major product of the disproportionation reaction.

Fig. 5 shows the resistance and desorption behaviour on reheating the disproportionated mixture under vacuum. The changes in resistivity correspond to the desorption events. The first desorption as indicated by pressure changes starts around 200 °C, a second around 250 °C overlapping with the former. Both describe the transition of $NdH_{\sim 2.7}$ to $NdH_{\sim 2}$ in the neodymium-rich phase and the disproportionated matrix phase, respectively [14]. Around 600 °C the constituents start to recombine to form the $Nd_2Fe_{14}B$ phase, thus causing an increase in resistivity.

Microstructural characterization [15] has shown that the material is fully disproportionated when a constant, equilibrium resistivity is attained and the same applies for the recombination reaction. The resistivity data of Fig. 3 indicate that the $Nd_{16}Fe_{76}B_8$ alloy is fully disproportionated after 19 ± 2 min exposure to hydrogen at $p(H_2) = 0.7$ bar and fully recombined after 20 ± 2 min desorption at $T = 800$ °C. The corresponding times for the stoichiometric $Nd_2Fe_{14}B$ alloy are 29 ± 2 and 71 ± 2 min, respectively, (for identical sample thicknesses of $t = 0.8$ mm). Thus, both reactions are much slower for the stoichiometric alloy. These changes in resistivity correlate with the hydrogen absorption and desorption pressure behaviour. The slightly smaller quantity of hydrogen absorbed in the stoichiometric $Nd_2Fe_{14}B$ alloy can be attributed to the absence of neodymium-rich phase in this material [16].

These studies indicate that the neodymium-rich grain-boundary phase has a significant influence on the kinetics of the HDDR reactions. It was reported earlier [8] that the hydrogen diffuses either in the hydrided neodymium-rich phase or at the interface between this phase and the matrix phase. It was shown [8] that the disproportionation reaction begins at the neodymium-rich/$Nd_2Fe_{14}B$ boundaries and proceeds towards the centre of the original grains. For the stoichiometric $Nd_2Fe_{14}B$ alloy, no such fast transport paths exist, which could explain the lower reaction rates in this material.

A detailed presentation of the disproportionation and recombination reactions in an homogenized $Nd_{16}Fe_{76}B_8$ alloy are given in Figs 6 and 7, respectively. The completion times for the two reactions are comparable to that of the as-cast $Nd_{16}Fe_{76}B_8$ alloy. The initial kink (Fig. 6) soon after the introduction of hydrogen, due to the hydrogenation of the intergranular phase, is more pronounced when compared with that of the as-cast material and this can be attributed to a more homogeneous distribution of this phase in the matrix phase. Different slopes in the resistivity curve corresponding to slope changes in the desorption curve represent the various stages during the recombination reaction. At point A in Fig. 7, the neodymium-hydride of the disproportionated mixture dissociates into neodymium metal which then

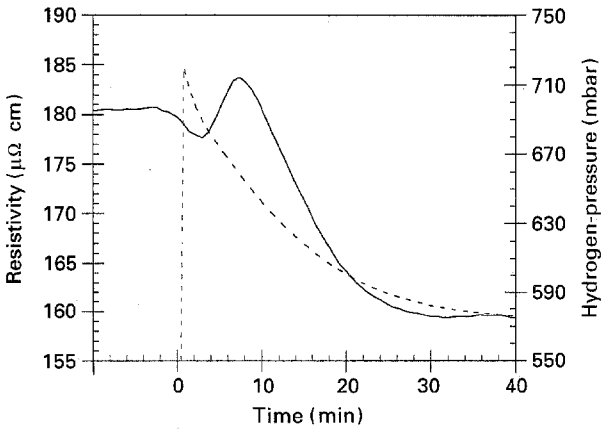


*Figure 6* Detailed presentation of the disproportionation reaction in a homogenized $Nd_{16}Fe_{76}B_8$ alloy monitored by the (——) resistance and (– – –) absorption behaviour; hydrogen introduction at $t = 0$ min.

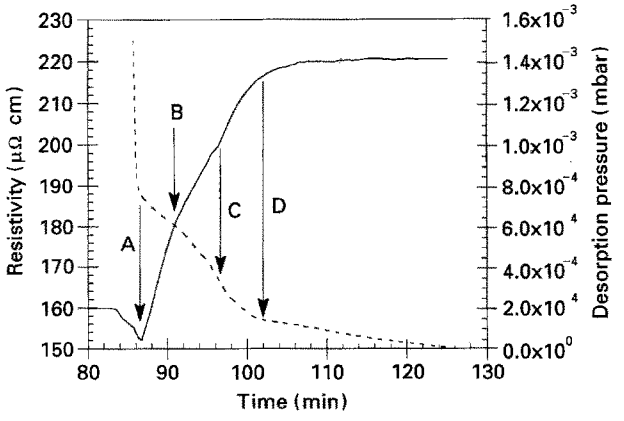


*Figure 7* Detailed presentation of the recombination reaction in a homogenized $Nd_{16}Fe_{76}B_8$ alloy monitored by the (——) resistance and (– – –) desorption behaviour; evacuation of the system at $t = 84$ min.

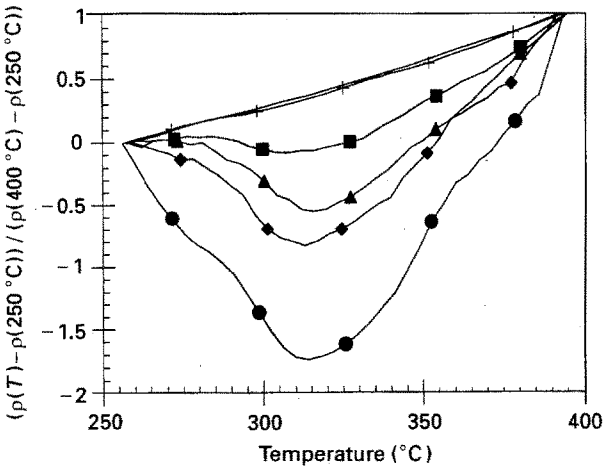


*Figure 8* Ratio of $(\rho(T)-\rho(250\,°C))/(\rho(400\,°C)-\rho(250\,°C))$ versus temperature monitoring the development of the Curie-point of an as-cast $Nd_{16}Fe_{76}B_8$ alloy for different stages of recombination at $T = 620\,°C$. (——) 0 h, ( + ) 2 h, (■) 6 h, (▲) 10 h, (◆) 14 h, (●) 18 h.

recombines with the other constituents. Points B and C could represent intermediate stages in the recombination reaction [9, 17]. The increase in resistivity is indicative of the consumption of α-Fe and the corresponding re-formation of the $Nd_2Fe_{14}B$ matrix phase. At point *D* the recombination reaction is completed.

## 3.4. Low-temperature recombination

Controlled recombination at $T = 620\,°C$ was achieved by monitoring the hydrogen desorption behaviour and the development of the Curie-point resistance anomaly of the re-formed $Nd_2Fe_{14}B$ matrix phase. At this temperature, the desorption of the hydrided neodymium-rich grain-boundary phase does not occur and hence melting of the grain-boundary material is avoided. The observed changes in resistivity will now be derived entirely from transformations within the matrix phase. The disproportionated material was cooled under hydrogen to room temperature and reheated to $T = 620\,°C$ under vacuum to desorb for 2 h and then cooled again, this cycle being repeated until the material was fully recombined. The equilibrium resistivity was reached when the material was fully desorbed. At conventional HDDR processing temperatures (750–850 °C) it can be assumed that the neodymium-rich grain-boundary phase re-melts after the hydrogen is fully desorbed, whereas at $T = 620\,°C$ the microstructural changes will occur in a solid–solid reaction because the neodymium-rich grain-boundary phase remains in the solid, hydrided state. The development of the Curie-point anomaly by evaluating the resistivity data during the heating stage of the cycling procedure described above is shown in Fig. 8. The ratio $(\rho(T) - \rho(250\,°C))/(\rho(400\,°C) - \rho(250\,°C))$ is plotted over the temperature range $T = 250$–$400\,°C$. At $T = 620\,°C$, the different stages during recombination can be monitored and the amount of re-formed $Nd_2Fe_{14}B$ matrix phase can be estimated, because the observed changes are due to transformations in the matrix phase. After 18 h at $T = 620\,°C$, no further changes occur and therefore it can be assumed that the material is fully recombined. The pattern in the overall

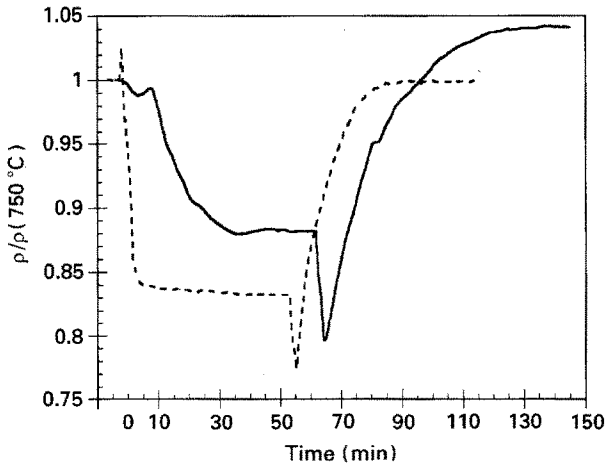


*Figure 9* Isothermal part of electrical resistivity versus time, monitoring the (——) first and (– – –) second HDDR cycle at $T = 750\,°C$ and $p(H_2) = 0.7$ bar of a $Nd_{16}Fe_{76}B_8$ alloy.

resistivity behaviour is similar to that of a stoichiometric alloy at $T = 800\,°C$.

## 3.5. The effect of cycling on the HDDR kinetics

If the grain-boundary phase acts as a diffusion path for the hydrogen, then a faster disproportionation in the material with the finer grain size would be anticipated. Previous work [12] in this laboratory using thermopiezic analysis has shown that the disproportionation temperature is lowered in fine-grain material.

In Fig. 9 a first and a second cycle of an S-HDDR process at 750 °C and $p(H_2) = 0.7$ bar in a $Nd_{16}Fe_{76}B_8$ alloy are shown. After the first cycle the material has a submicrometre grain size causing the acceleration of the disproportionation reaction in the second cycle, which appears now to be almost instantaneous As the hydrogen diffusion into the matrix phase is

much more rapid, the initial kink due to the hydrogenation of the neodymium-rich phase is much sharper for the second cycle. Moreover, it is interesting to note that the equilibrium resistivity after disproportionation is at a lower level for the second cycle. The recombination reaction in the second cycle is completed slightly earlier which could be attributed to a refinement of the microstructure of the disproportionation product. This possibly new phenomenon might effect the microstructure of the recombined material and remains the subject of further investigation. The value of resistivity after recombination, compared with that before disproportionation, remains on a similar level which is consistent with the unchanged grain size for the second cycle. The kinetics of any subsequent cycle do not differ significantly to those of the second cycle.

## 3.6. The effect of hydrogen pressure on the HDDR kinetics

The effect of hydrogen pressure ($p(H_2) = 0.1$–$1.0$ bar) on the kinetics of the disproportionation reaction was investigated at 750 °C in a $Nd_{14.68}Dy_{0.94}Al_{0.62}Fe_{76.47}Nb_{0.5}B_{6.79}$ alloy. Second and subsequent HDDR cycles were recorded to ensure that the grain size before and after the HDDR process was comparable. It was observed that the disproportionation reaction was accelerated when the hydrogen pressure increased, whereas the recombination reaction remains unaffected by the initial hydrogen pressure. Moreover it can be concluded from Fig. 10 that the equilibrium resistivity after the completion of disproportionation reaction is very sensitive to the amount of hydrogen stored in the sample. A different neodymium hydride is formed, depending on the hydrogen pressure in the system. Increased hydrogen pressure results in a larger H/Nd ratio which increases the equilibrium value of resistivity. The minimum resistivity can be found when the system is evacuated; the neodymium hydride dissociates at this stage. However, this process overlaps with the recombination reaction resulting in a subsequent increase in resistivity. Interrupting the recombination process by reintroducing hydrogen to the same pressure establishes the same equilibrium values. The decrease in resistivity for lower hydrogen pressure can be attributed to the fact that the hydrogen deficient rare-earth di-hydrides ($REH_{1.8}$ to $REH_{1.9}$) are actually better electrical conductors than the corresponding rare-earth metals [18]. Moreover, for hydrogen concentrations in excess of the di-hydride composition, a sharp increase in equilibrium resistivity can be expected [18]. For neodymium hydride, Heckman and Hills [19] reported a maximum conductivity at $NdH_{1.9}$. It should be noted that there is a linear relationship between the equilibrium resistivity and $p(H_2)^{0.5}$, described by Sieverts' law, which is illustrated in Fig. 11. This indicates a probable linear relationship between the electrical resistance and the hydrogen content in the neodymium hydride over this range of compositions.

The rates of the disproportionation reaction versus time at 750 °C for various hydrogen pressures are shown in Fig. 12. The maximum reaction rate for $p(H_2) = 0.7$ bar can be estimated as being ten times

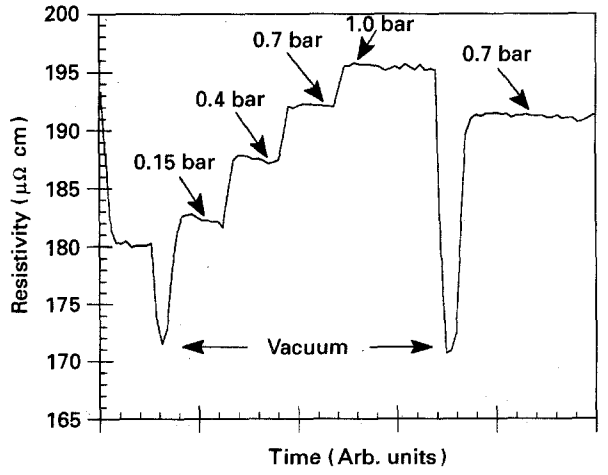


*Figure 10* Equilibrium resistivity of the fully disproportionated material for different hydrogen pressures ($p(H_2) = 0.1$–$1.0$ bar) at $T = 750$ °C.

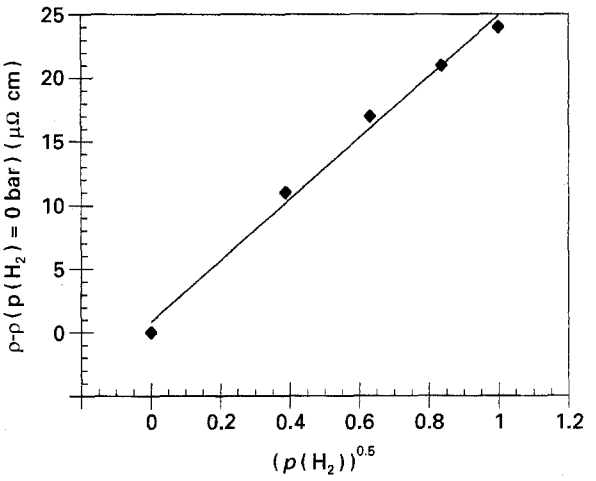


*Figure 11* Sieverts' law applied for a disproportionated mixture under various hydrogen pressures.

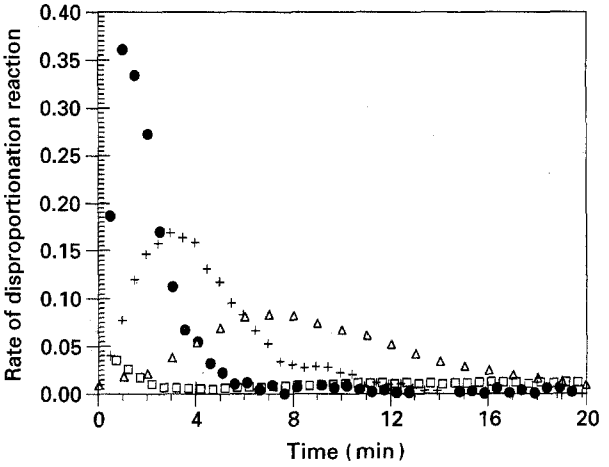


*Figure 12* Rate of the disproportionation reaction versus time at $T = 750$ °C for various hydrogen pressures; (●) 1 bar, ( + ) 0.7 bar, (△) 0.35 bar, (□) 0.2 bar.

higher than that for $p(H_2) = 0.2$ bar. Moreover, the times where the maxima occur are very dependent on the hydrogen pressure. These results elucidate clearly the basic role of hydrogen pressure in the disproportionation process; consistent with a strong dependence of the equilibrium pressure of $NdH_{\sim 2}$ on temperature [20]. Thus, it can be used as an effective and sensitive means of controlling and optimizing the overall process.

## 3.7. Onset of disproportionation and recombination

The electrical resistivity and the hydrogen desorption behaviour of a disproportionated $NdH_{\sim 2}$, α-Fe, $Fe_2B$ mixture between $T = 750$ and 1000 °C under an initial pressure of $p(H_2) = 35$ mbar is shown in Fig. 13. The measurements revealed the Curie-point resistance anomaly of α-Fe at $T = 770 \pm 5$ °C and a major desorption at $T = 810 \pm 5$ °C causing another change in slope in the resistivity curve. This event can be interpreted as recombination under a hydrogen atmosphere. It was observed that the higher the pressure, the higher was the temperature for the desorption event. The pressure changes at higher temperatures can be attributed to the desorption of the neodymium-rich grain-boundary phase [14] and this corresponds with a fall in the resistivity.

Starting from a recombined material, the hydrogen pressure was increased step by step and the "equilibrium" resistivity was measured at different isotherms. It was found that the resistivity of the 2–14–1-hydride exhibited a Sieverts'-type behaviour before the sharp onset of the disproportionation reaction. These studies indicate that the start of the disproportionation and recombination reactions depend critically on the stability of $NdH_{\sim 2}$, which is determined by hydrogen pressure and processing temperature, as shown in Fig. 14. A hysteresis effect [21] for the $NdH_{\sim 2}$, was observed because the data for the onset of disproportionation and recombination were derived from absorption and desorption isotherms, respectively.

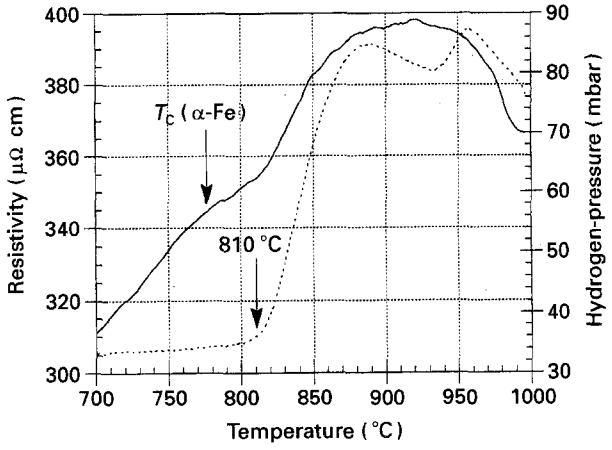


*Figure 13* (——) Electrical resistivity and (– – –) hydrogen desorption behaviour between $T = 750$ and 1000 °C under an initial pressure of $p(H_2) = 35$ mbar of a disproportionated $NdH_{\sim 2}$, α-Fe, $Fe_2B$ mixture.

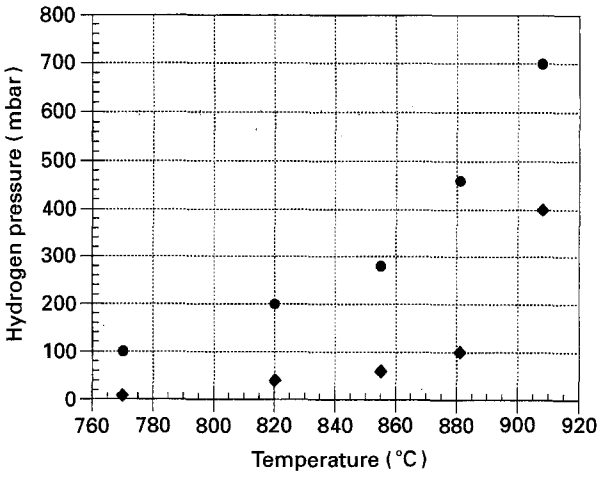


*Figure 14* Onset of (●) disproportionation and (◆) recombination under a hydrogen atmosphere in the temperature range $T = 770$–910 °C for a $Nd_{16}Fe_{76}B_8$ alloy.

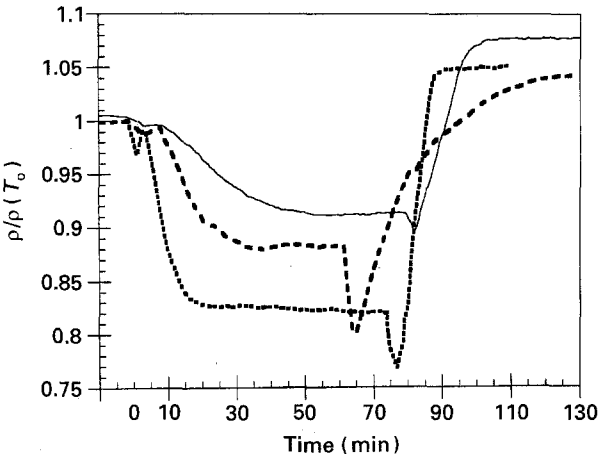


*Figure 15* Isothermal part of electrical resistivity versus time monitoring the HDDR process at $T =$ (– – –) 750, (---) 800 and (——) 860 °C and $p(H_2) = 0.7$ bar for a $Nd_{16}Fe_{76}B_8$ alloy.

## 3.8. The effect of temperature

The effect of temperature on the disproportionation and the recombination stage of the HDDR process was investigated on a $Nd_{16}Fe_{76}B_8$ alloy, which was exposed to a hydrogen pressure of $p(H_2) = 0.7$ bar at various temperatures. Fig. 15 shows the overall process for three typical temperatures ($T = 750$, 800 and 860 °C). In Fig. 16 it can be seen how the completion time (taken when resistivity is constant) of the disproportionation and recombination reactions varies in a temperature range of $T = 620$–900 °C. With increasing temperature the neodymium-hydride becomes more and more unstable [20], whereas the thermally activated bulk diffusion will increase continuously, resulting in a maximum disproportionation reaction rate around 810 °C. The recombination reaction rate increases with the processing temperature, as only thermally activated bulk diffusion processes have to be taken into account. As described above, below 650 °C the intergranular phase is in the hydrided and

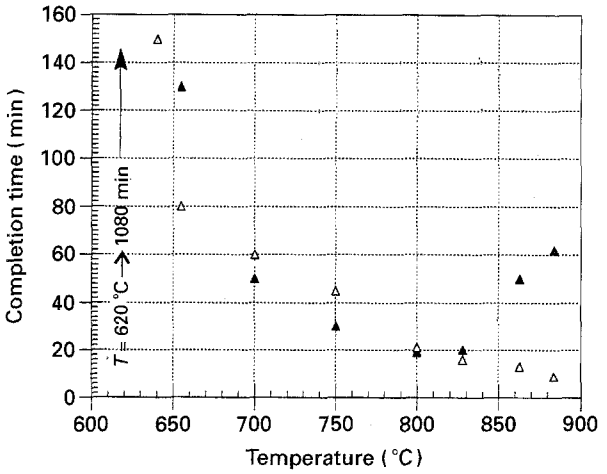


*Figure 16* Completion time of the (▲) disproportionation and (△) recombination reaction for a temperature range $T = 620$–$885\,^{\circ}C$ for a $Nd_{16}Fe_{76}B_8$ alloy.

solid state causing a sharp increase in recombination time; for 655, 640 and 620 °C the corresponding times are 80, 150 and 1080 min, respectively.

It can be concluded, that it is the stability of $NdH_{2\pm x}$ which determines to a great extent the HDDR disproportionation and recombination stages. At high temperatures, although the reaction is exothermic, large entropy contributions have to be compensated by high hydrogen pressures to start the disproportionation reaction. On the other hand, lowering the hydrogen pressure in the disproportionated state will initiate the recombination reaction under a hydrogen atmosphere, if the temperature is sufficiently high. This observation is consistent with work by Takeshita and Nakayama [22], who reported on the basis of $X$-ray diffraction measurements, that the disproportionated mixture will recombine above 1000 °C under a hydrogen pressure of 1 bar.

## 4. Conclusions

It has been shown that *in situ* electrical resistivity measurement is a highly suitable method of investigating details of the S-HDDR process in Nd–Fe–B-type alloys. A more fundamental understanding of the reaction mechanisms and kinetics depending on parameters such as alloy composition, hydrogen pressure and processing temperature, has been achieved. It was found that

1. the neodymium-rich intergranular material has a marked influence on the disproportionation and recombination reactions; the amount and the state, solid or liquid, of the phase will determine the kinetics; much slower kinetics are observed for the recombination process when the neodymium-rich material is in the solid state;

2. a smaller grain size of the $Nd_2Fe_{14}B$ matrix phase will accelerate the disproportionation reaction;

3. the disproportionation reaction is very sensitive to the applied hydrogen pressure;

4. the onset of the disproportionation and recombination depends critically on the stability of the neodymium hydride, which is determined by pressure and temperature;

5. the balance between the stability of the neodymium-hydride and thermally activated bulk diffusion determine the rate of the disproportionation reaction exhibiting a maximum around 810 °C under a pressure of $p(H_2) = 0.7$ bar for a $Nd_{16}Fe_{76}B_8$ alloy.

## Acknowledgements

The authors thank the European Commission for the provision of a fellowship (O.G.), and SERC and CEAM for support of the general research programme of which the work forms part. M. Verdier is thanked for stimulating discussions.

## References

1. F. GENCER and I. R. HARRIS, *J. Mater. Sci.* **26** (1991) 6625.
2. O. GUTFLEISCH, M. VERDIER, I. R. HARRIS and A. E. RAY, *IEEE Trans. Magn.* **29** (1993) 2872.
3. O. GUTFLEISCH, M. VERDIER and I. R. HARRIS, *J. Alloys Compos.* **196** (1993) L19.
4. F. AHMED, O. GUTFLEISCH and I. R. HARRIS, *IEEE Trans. Magn.* **30** (1994) 616.
5. I. R. HARRIS, in "Proceedings of the 12th International Workshop on Rare-Earth Magnets and their Applications", University of Western Australia, Canberra, Australia (1992) p. 347.
6. T. TAKESHITA and R. NAKAYAMA, *ibid.*, p. 67.
7. P. J. McGUINESS, E. J. DEVLIN, I. R. HARRIS, E. ROZENDAAL and J. ORMEROD, *J. Mater. Sci.* **24** (1989) 2541.
8. O. GUTFLEISCH, N. MARTINEZ, M. VERDIER and I. R. HARRIS, *J. Alloys Compos.* **204** (1994) L21.
9. O. GUTFLEISCH, M. MATZINGER, J. FIDLER, N. MARTINEZ and I. R. HARRIS, in "Proceedings of the 8th International Symposium on Magnetic Anisotropy and Coercivity in Rare-Earth-Transition Metal Alloys", Birmingham, UK, September 1994, p. 243.
10. C. MUELLER, B. REINSCH and G. PETZOW, *Z. Metallkd.* **83** (1992) 845.
11. G. SCHNEIDER, E. T. HENIG, G. PETZOW and H. H. STADELMAIER, *ibid.* **77** (1986) 755.
12. D. BOOK and I. R. HARRIS, *IEEE Trans. Magn.* **28** (1992) 2145.
13. X. J. ZHANG, P. J. McGUINESS and I. R. HARRIS, *J. Appl. Phys.* **69** (1991) 5838.
14. D. BOOK and I. R. HARRIS, in "Proceedings of the 8th International Symposium on Magnetic Anisotropy and Coercivity in Rare-Earth-Transition Metal Alloys", Birmingham, UK, September 1994, p. 205.
15. O. GUTFLEISCH, N. MARTINEZ, M. VERDIER, and I. R. HARRIS, *J. Alloys Compos.*, **215** (1994) 227.
16. P. J. McGUINESS, I. R. HARRIS, U. D. SCHOLZ and H. NAGEL, *Z. Phys. Chem. Neue Folge* **163** (1989) 687.
17. N. MARTINEZ, D. G. R. JONES, O. GUTFLEISCH, D. LAVIELLE, D. PERE and I. R. HARRIS, in "6th MMM-Intermag Conference 1994", Albuquerque, New Mexico, USA, *J. Appl. Phys.* to be published.
18. K. A. GSCHNEIDNER and LEROY EYRING, "Handbook on the Physics and Chemistry of Rare Earths, Vol. 3 (North-Holland, Amsterdam, 1979) p. 229.
19. R. C. HECKMAN and C. R. HILLS, *Bull. Am. Phys. Soc.* **10** (1965) 126.
20. C. OHKI, H. UCHIDA and E. KO, *J. Jpn Inst. Metals* **54** (1990) 146.
21. K. H. J. BUSCHOW, P. C. P. BOUTEN and A. R. MEIDEMA, *Rep. Prog. Phys.* **45** (1982) 937.
22. T. TAKESHITA and R. NAKAYAMA, in "Proceedings of the 11th International Workshop on Rare-Earth Magnets and their Applications", Pittsburgh, PA, edited by S. G. Sankar, Carnegie Mellon University (1990) p. 49.

*Received 8 September*
*and accepted 4 October 1994*